Thu hồi vật liệu từ pin sơ cấp thải: ảnh hưởng của graphene đến cấu trúc và tính chất quang của composite ZnO

TÓM TẮT

Pin sơ cấp đặc biệt là pin alkaline and Zn-C được sử dụng phổ biến trong các thiết bị điện tử gia dụng nhưng có vòng đời ngắn, chỉ dùng một lần và đang trở thành nguồn rác thải điện tử nguy hại nếu không được xử lý đúng cách. Trong nghiên cứu này, ba composite ZnO/X với chất nền X = graphene, graphitic carbon (g-C_3N_4), and graphene-graphitic carbon (graphene/g-C_3N_4) đã được tổng hợp bằng phương pháp thuỷ nhiệt với nguồn nguyên liệu ban đầu Zn, và C được thu hồi từ pin sơ cấp Panasonic AA thải. Kết quả của phương pháp kính hiển vi điện tử quét (SEM), nhiễu xạ tia X (XRD), hồng ngoại biến đổi Fourier (FT-IR), quang phổ điện tử tia X (XPS), phổ tán xạ năng lượng tia X (EDS) và phổ phản xạ khuếch tán UV-Vis DRS đã làm rõ vai trò của graphene ảnh hưởng lớn đến: (i) khả năng hình thành tinh thể ZnO trên các vật liệu nền, (ii) cấu trúc bề mặt vật liệu đã làm giảm khả năng kết tụ các hạt ZnO, (iii) cải thiện khả năng hấp thụ ánh sáng khả kiến của vật liệu. Ảnh hưởng của graphene đến vật liệu composite được khẳng định thông qua phản ứng phân huỷ kháng sinh rifampicin trong vùng ánh sáng khả kiến.

Từ khóa: *Thu hồi pin sơ cấp thải, composite ZnO, ảnh hưởng graphene.*

Recycling of spent primary batteries: the role of graphene in ZnO-based photocatalysts

ABSTRACT

Primary batteries, particularly alkaline and zinc–carbon (Zn-C) types, have a relatively short service life and are frequently discarded in landfills, leading to potential environmental risks and health concerns. In order to overcome these challenges, herein, we synthesize three photocatalyst composites ZnO/X by coupling ZnO with X = graphene, graphitic carbon (g-C_3N_4), and graphene-graphitic carbon (graphene/g-C_3N_4) substrates using a hydrothermal method with ZnO, and graphene is recovered from spent primary Panasonic AA batteries as the Zn and C source. Techniques such as scanning electron microscopy (SEM), X-ray diffraction (XRD), and Fourier Transform infrared (FT-IR), X-ray photoelectron spectroscopy (XPS), and diffuse reflectance ultraviolet-visible spectroscopy (UV-vis DRS) have been employed to elucidate the strong influence of graphene on the crystal structure, surface morphology, optical characteristics, and photocatalytic performance of the synthesized composites.

Keywords: *Recovery spent primary batteries, composite ZnO-based, influence of graphene.*

1. INTRODUCTION

The increasing amount of spent batteries, including non-rechargeable and lithium-ion batteries, is a key factor contributing to environmental pollution and health issues. Recently, considerable attention has been given to the recycling of spent primary batteries to recover valuable secondary resources such as Zn, Mn, and graphite, which serves as an effective approach to minimizing risks and mitigating environmental impacts at the end of life.[1-3]

As a metal oxide semiconductor, ZnO possesses properties such as excellent chemical stability, strong oxidizing capability, and cost-effective production, offering broad application prospects. However, ZnO absorbs only a limited amount of sunlight and undergoes photoexcited electron–hole recombination due to its large band gap.[4] Consequently, considerable efforts have been made to enhance its optical absorption and photocatalytic activity under illumination with visible light, for example by combining ZnO with graphene or g-C_3N_4.[5-7] Nevertheless, the effect of substrate on the structural and optical properties of ZnO-based composites remains unclear. Additionally, comparing the degradation efficiency of rifapicin antibiotic (Rif) under LED light is a practical approach to exploring the role of graphene in boosting the photocatalytic efficiency of ZnO/graphene, ZnO/g-C_3N_4, and ZnO/graphene/g-C_3N_4.

Synthesis of composites ZnO/X (X = graphene; g-C_3N_4; graphene-g-C_3N_4)

- *The substrate X:* graphene synthesized from graphite foil of spent Panasonic AA 1.5 V batteries through modified Hummer's method. In brief, the cell case was carefully dismantled, and the carbon rod was collected and subsequently washed with distilled water to eliminate residual

This work aims to develop a sustainable approach for synthesizing ZnO-based materials from alkaline battery waste, with subsequent applications in photocatalytic reactions. In particularly, the influence of graphene is clarified through various characterization techniques, which reveal its effects on the crystallinity of ZnO on the supporting substrate, the surface morphology, and the visible-light absorption properties. The ZnO/graphene composite exhibits significantly improved photocatalytic performance, with a degradation efficiency of approximately 41% of Rif removed after 60 min of irradiation, which is 1.5 and 1.7 times higher than that of ZnO/graphene/g-C_3N_4 and ZnO/g-C_3N_4, respectively.

2. EXPERIMENT

2.1. Material synthesis process

Chemicals

Spent primary Zn-C batteries (Panasonic AA 1.5 V) were collected locally from Gia Lai province. Sulfuric acid (H_2SO_4, 98%), sodium nitrate ($NaNO_3$), hydrochloric acid (HCl, 36.5%), hydrogen peroxide (H_2O_2, 30%), potassium permanganate ($KMnO_4$, 99%) were received from Xilong, China. Melamine ($C_3H_6N_6$, 99%), and rifampicin (95%) were Sigma-Aldrich, Germany.

electrolytes. The graphite foils were initially washed with distilled water, dried, ground, and sieved to obtain graphite powder, which served as the precursor for graphene synthesis. Graphene powder was then produced using the modified Hummer's method, while g-C_3N_4 was prepared through the solid-state reaction of melamine.[8] Finally, the g-C_3N_4/graphene composite was fabricated via a hydrothermal process, following the procedure reported in our earlier works.[9]

- The *ZnO/X* ***(X = graphene; g-C_3N_4; graphene-g-C_3N_4)*** composites (Scheme 1) were hydrothermally synthesized in ethanol from a dispersed mixture of as-synthesized *substrate X* and $ZnCl_2$ solution, which was leached from the Zn case of spent primary Panasonic AA 1.5 V batteries with HCl 5% acid. Specifically, 0.5 g of substrate X powder was dispersed to 100 mL of ethanol and stirred for 1 h with a magnetic stirrer to form a homogeneous suspension. Subsequently, 2 mL of $ZnCl_2$ solution was slowly introduced and stirred for an additional 2 h. The mixture was then transferred into a Teflon-lined autoclave and heated at 180 °C for 8 h. The resulting product was centrifuged, thoroughly washed with distilled water and ethanol until neutral pH was reached, dried in air at 80 °C for 12 h, and finally calcined at 300 °C for 2 h. The obtained samples were denoted as ZG, ZN, and ZGN, respectively.

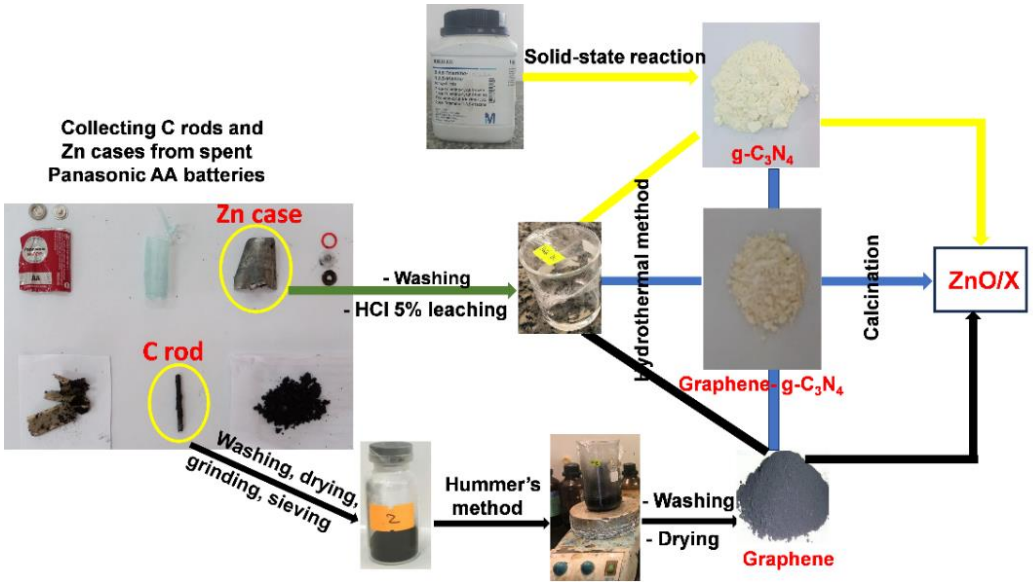

Scheme 1. Illustration of the synthesis reaction for ZnO/X preparation

Materials characterization

The crystalline structure was determined by powder X-ray diffraction (Bruker D2 Advance) with Cu-Kα radiation (λ = 0.154 nm), and diffraction data were collected within a 2θ range of 10 – 70°. Elemental compositions and chemical states were examined by X-ray photoelectron spectroscopy (XPS), with binding energy values referenced to the adventitious carbon C 1s peak at 284.8 eV. Fourier-transform infrared (FT-IR) spectra were recorded on a Shimadzu FTIR-Iffranity-1S spectrometer (S/N ratio 30000:1) using KBr pellets containing 1 wt% of sample. The morphology and elemental compositions of the obtained materials were analyzed using scanning electron microscopy combined with EDS (SEM, HITACHI S-4800). Optical properties were investigated by UV-Vis diffuse reflectance spectra (DRS) were measured with a Scinco S-4100 spectrophotometer, and absorption spectra were obtained using a Shimadzu UV-1800 instrument.

Photocatalytic study: The photocatalytic activity of the synthesized ZnO/X materials was evaluated by the degradation of Rifapicin antibiotic. Rif was prepared in a fixed concentration (20 mg/L), and the prepared solution was allowed to settle in the dark for 10 hours. To evaluate the photocatalytic activity, 20 mg of catalyst was dispersed in 80 mL of Rif solution contained in a 250 mL flask and kept in the dark box. The suspension was magnetically stirred for 1 hour to establish adsorption–desorption equilibrium. Afterwards, the solution was exposed to visible light irradiation from an LED lamp (30 W). At every 10-minute interval, 5 mL of the suspension was collected and centrifuged to separate the catalyst. The remaining Rif concentration in the supernatant was analyzed by a photometric colorimetric method using a Shimadzu 1800 spectrometer.

3. RESULTS AND DISCUSSION

As shown in Figure 1a, the diffraction peaks of the ZG composite appearing at 2θ = 31.7, 34.4, 36.2, 47.5, 56.6, 62.9, and 66.3° are indexed to the (100), (200), (101), (102), (110), (103), and (113) lattice planes of ZnO, which are consistent with the standard JCPDS card No. 36-1451. Moreover, the XRD pattern of the ZG sample shows an additional broadened diffraction peak at 2θ = 25.9° besides the peaks assigned to ZnO, which is the characteristic peak of the (002) plane of graphene.[10] However, comparing the XRD curves of the ZN and ZGN composites with those of ZG, it can be observed that the major peaks are identical to those of g-C_3N_4 at 12.7 and 27.1°. And the inconsiderable ZnO-related peaks could be clarified due to the low content of this component. The XRD pattern analysis indicates that the graphene substrate can produce more formation of well-crystallized ZnO, while C_3N_4 likely interacts more strongly with Zn^{2+}, suppressing crystallization, resulting in poorly crystalline ZnO nanoparticles that are similar to our observed previous findings on TiO_2-based composites.[8,11]

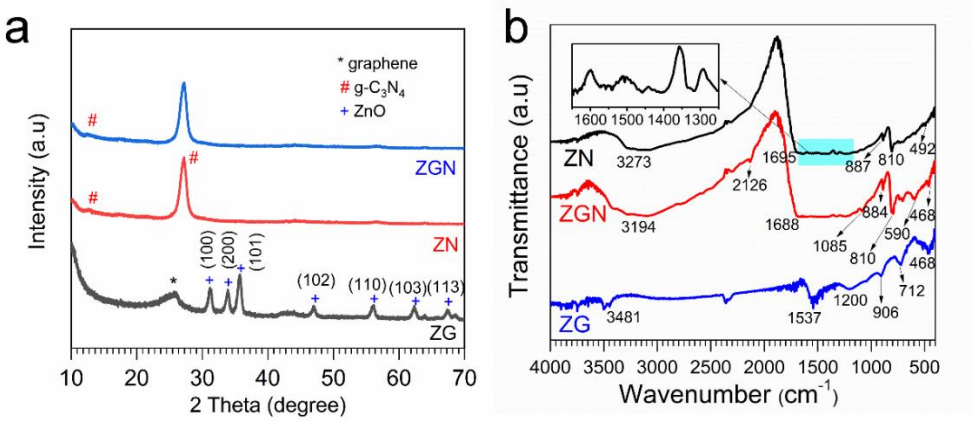

Figure 1. XRD patterns (a) and FTIR spectra (b) of the as-prepared ZG, ZN, and ZGN samples.

FTIR analysis was performed to identify the bond groups and displayed in Fig. 1b. For ZG, the characteristic bands at 468 cm^{-1} are attributed to Zn–O vibrations, while the broad band around 3481 cm^{-1} is associated with O–H stretching of surface hydroxyl groups. The absorption peaks located at 1537 cm^{-1} and 1200–906 cm^{-1} can be assigned to C–H and C–O stretching, respectively. In the cases of ZN and ZGN, the broad band in the region of 3194-3273 cm^{-1} originates from N–H vibrations and O-H of adsorbed H_2O molecules. The intense peak at 810 cm^{-1} corresponds to the out-of-plane bending of the s-triazine ring in g-C_3N_4. Moreover, the characteristic bands of CN heterocycles and C–N–C groups between 1250 and 1630 cm^{-1} overlap into a broad band, which becomes more pronounced upon ZnO crystallization, which Anshu Sharma et. al also observes.[12] Additionally, the weak Zn–O stretching vibrations at 468 cm^{-1} (for ZGN) and 492 cm^{-1} (for ZN) possibly resulted from the low amount of ZnO, which is in good agreement with XRD data.

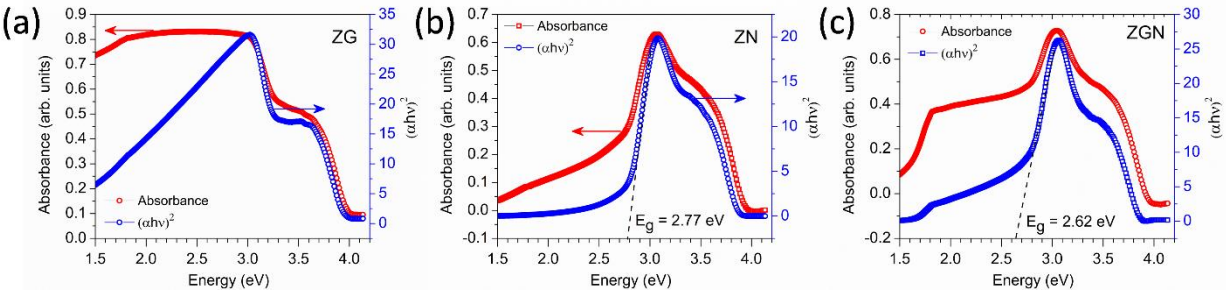

Figure. 2. UV-Vis DRS and the associated Tauc plots of ZN (a), ZN (b) and ZGN (c).

The UV–vis diffuse reflectance spectra were recorded to investigate the optical characteristics of the composite and their corresponding Tauc plots[13] were used, and the obtained results are shown in Fig. 2. As expected, the ZG sample (Fig. 2a) exhibits absorption in the visible region, which can be attributed to the incorporation of graphene into ZnO. For ZN, a bandgap of 2.77 eV is obtained, which is shown in Fig. 2b, while the bandgap is 2.62 eV for ZGN (Fig. 2c). Therefore, it is noticeable that a narrower bandgap is obtained for ZGN due to the contribution of graphene in the

composite. These results indicate that the incorporation of graphene enhances visible light absorption in the composite, potentially altering the fundamental mechanism of electron–hole pair generation under irradiation.

The SEM-EDS analysis investigated the morphology and surface elements of the as-synthesized composites, as shown in Fig. 3. Distinct morphologies of the ZG, ZN, and ZGN composites were observed, highlighting the influence of graphene incorporation on particle dispersion and surface structure. Fig. 3a shows ZnO/graphene with a wrinkled appearance with multiple folds. These highly crumpled structures offer a large surface area and facilitate the uniform anchoring of ZnO nanoparticles. The intimate contact between ZnO and graphene may promote effective interfacial charge transfer and suppress particle agglomeration, which are essential for enhancing photocatalytic activity. Additionally, the EDS analysis of the ZG sample (Fig. 3b) reveals that the major elements are C, O, and Zn, while minor and trace elements such as Ca, Cl, Si, Na, Al, and S are also detected. The presence of these elements is attributed to the use of precursors derived from spent Panasonic AA primary batteries. In contrast, the ZN sample (Fig. 3c) exhibits a densely aggregated morphology, with irregularly shaped ZnO particles forming compact clusters, resulting in significant particle agglomeration and reduced dispersion. Although a two-dimensional lamella structure with wrinkles and irregular folding structure for ZGN (Fig. 3e) is still observed, which suggests partial retention of the graphene structure, the ZnO particles are less uniformly distributed compared to ZG. This indicates that the graphene content in ZGN is insufficient to completely suppress particle aggregation. Nevertheless, the morphology is improved relative to the ZN composite, implying a moderate enhancement in interfacia interactions. Notably, the Zn content in ZN (0.49 wt%) and ZGN (0.80 wt%) is significantly lower than that in ZG (7.4 wt%), suggesting that the incorporation of graphene components facilitates higher Zn loading in the ZG composite.

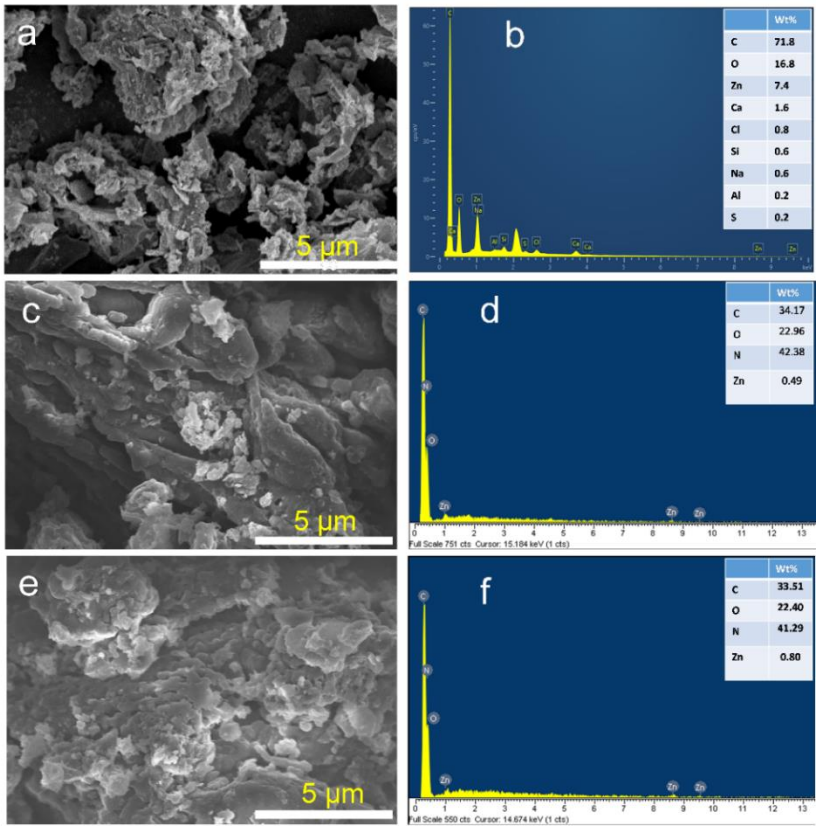

Figure 3. SEM image and EDS of ZG(a, b); ZN (c, d), and ZGN (e, f)

The surface chemical state of ZGN was investigated using the XPS technique. As shown in Fig. 4a, the XPS survey spectra include signals of Zn2p, Cl1s, O1s, N1s, and C1s corresponding to the composition of ZnO, graphene, and g-C_3N_4. The presence of fluorine in the composite, as indicated in the XPS survey spectrum, can be attributed to residual fluoride compounds derived from spent primary Panasonic AA batteries. According to Fig. 4b, the Zn 2p core-level of the ZnO spectrum has two peaks located at approximately 1044.1 and 1021.1 eV,

corresponding to the binding energies of Zn 2p3/2 and Zn 2p1/2, indicating that the chemical valence of Zn at the surface of ZnO is a +2 oxidation state. In the O 1s spectrum in Fig. 4c, three peaks are observed at 529.9. 531.2, and 532.0 eV can correspond to oxygen in the ZnO lattice (O_X), the oxygen vacancy in the ZnO lattice (O_V), and the OH groups attached to Zn^{2+} ions (O_{OH}), respectively. The C1s spectrum of ZGN indicates C-N-C at 287.3 eV, C=N/C=O at 286.7 eV, and N-C=N/O-C=O at 283.6 eV, respectively.

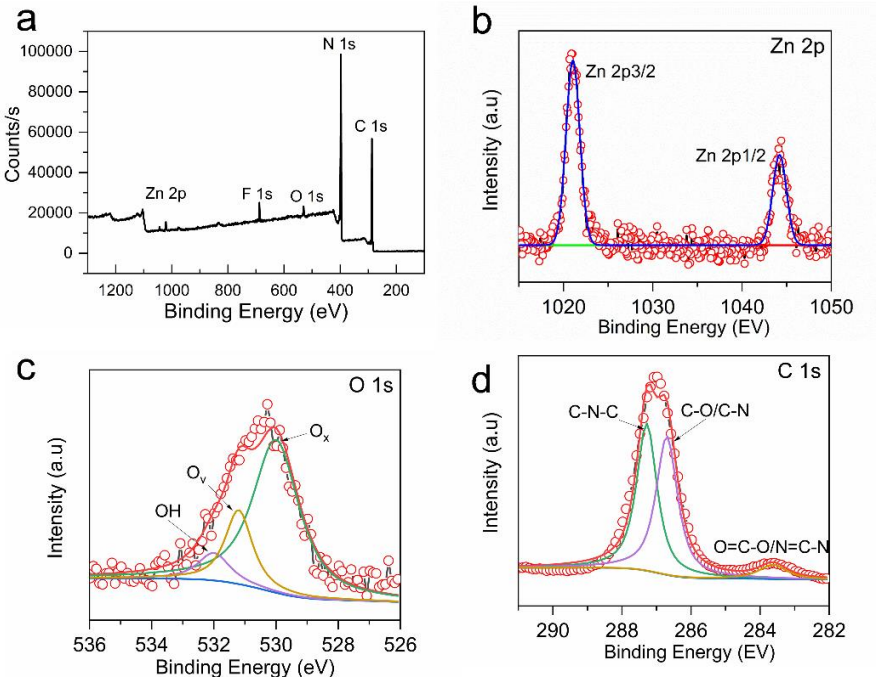

Figure 4. (a) XPS survey of ZGN composite (b) Zn 2p, (c) O1s, and (d) C1s spectral regions.

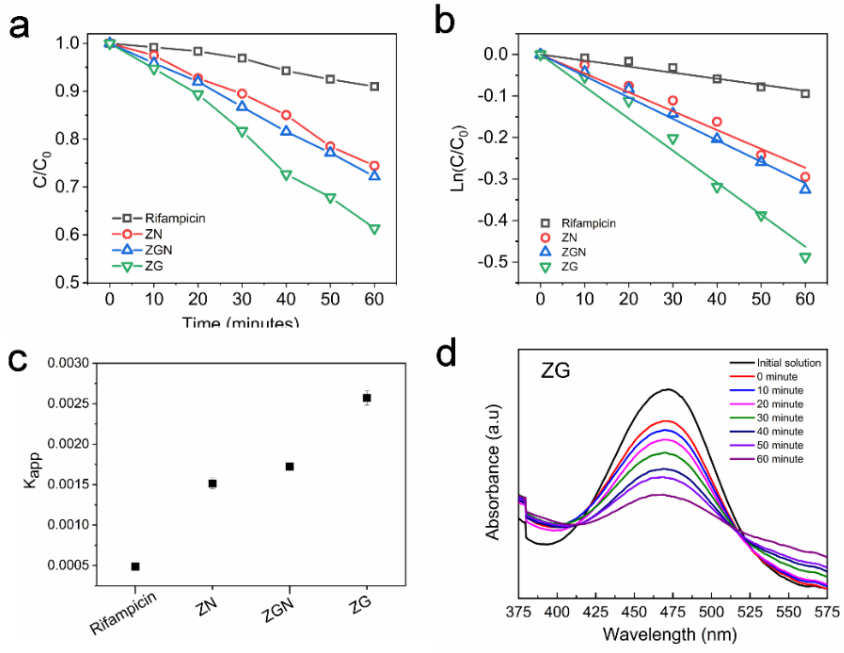

Fig. 5. Photocatalytic degradation of Rif in the presence of ZG, ZN, and ZGN photocatalysts (a); the degradation kinetic plots (b); the degradation rate (k_{app}) of Rif obtained for materials (c); and UV-vis absorption spectra of ZG for different irradiation times (d).

Fig. 5a shows the decrease of Rif concentration as a function of irradiation time by the photocatalysts, including ZN, ZGN, and ZG. In comparison, the concentration of Rif as a function of exposure time in the absence of a catalyst shows virtually no self-degradation. The results demonstrate that, after 60 minutes of light irradiation generated by the LED lamp, the ZN, ZGN, and ZG cause Rif degradation of

approximately 25.5%, 27.5%, and 41%, respectively. Additionally, the rate degradation of Rif by the highest photocatalytic activity is linked to its diminished kinetic characteristics for ZG, which exhibits 1.5 - 1.7 times higher activity than ZGN and ZN individually. The enhanced photocatalytic performance of the ZG can be attributed to improved kinetic properties resulting from the ZnO content control, the well-distributed and wrinkled graphene-based morphology, and enhanced visible light absorption achieved through the contribution of graphene.

4. CONCLUSION

In summary, three ZnO/X (X=graphene, g-C_3N_4, and graphene-g-C_3N_4) photocatalysts were prepared via a hydrothermal method using Zn, C recovered from spent primary batteries, and g-C_3N_4 from melamine. A comparative study has been conducted to demonstrate the role of graphene in the synthesis of ZnO-based photocatalysts. Although the amounts of precursors were similar (2 mL of $ZnCl_2$ solution and 0.5 g of substrate X) at the same synthesis conditions, it is revealed that the crystallization of ZnO on the substrate graphene became more favorable, improved particle dispersion, and enhanced visible light absorption, as confirmed by XRD, IR, SEM-EDS, and UV-Vis DRS. The photocatalytic efficiency of the synthesized materials under visible light exposure, evaluated by the degradation of the antibiotic rifampicin, was highest for the ZG composite, confirming the beneficial effect of graphene in the composite.

ACKNOWLEDGMENTS

TÀI LIỆU THAM KHẢO

[1] M. A. Salam, M. A. Gabal, and Y. M. Al Angari. The recycle of spent Zn-C batteries and the synthesis of magnetic nanocomposite from graphene nanosheets and ferrite and its application for environmental remediation, *J. Mater. Res. Technol.*, **2022**, *18*, 4267–4276.

[2] E. V. Beletskii, V. V. Pakalnis, D. A. Lukyanov, D. V. Anishchenko, A. I. Volkov, and O. V. Levin. Recycling spent graphite anodes into a graphite/graphene oxide composite via plasma solution treatment for reuse in lithium-ion batteries, *J. Environ. Chem. Eng.*, **2023**, *11 (1)*, 1-27.

[3] V. Valdrez, M. F. Almeida, and J. M. Dias. Direct recovery of Zn from wasted alkaline batteries through selective anode's separation, *J. Environ. Manage.*, **2022**, *321*, p. 115979.

[4] R. R. Wary *et al.*. Highly Oriented Nitrogen-Doped Flower-like ZnO Nanostructures for Boosting Photocatalytic and Photoelectrochemical Performance: A Combined Experimental and DFT Study, *J. Phys. Chem. Lett.*, **2025**, *16(20*), 5180–5187.

[5] T. Imboon *et al.*. Synergistic Effects of Fe-Doped ZnO and Graphene Oxide for Enhanced Photocatalytic Performance and Tunable Magnetic Properties, *ACS Omega*, **2025**, *XX*, XXX–XXX

[6] S. Pourali, R. Amrollahi, S. Alamolhoda, and S. M. Masoudpanah. In situ synthesis of ZnO/g-C_3N_4 based composites for photodegradation of methylene blue under visible light, *Sci. Rep.*, **2025,** *15(1)*, 1–13.

[7] M. H. Shakoor *et al.*. Enhancing the photocatalytic degradation of methylene blue with graphene oxide-encapsulated g-C_3N_4/ZnO ternary composites, *ACS omega*, **2024**, *9(14)*, 16187–16195.

[8] T. L. Thi Le *et al.*. Controlled growth of TiO_2 nanoparticles on graphene by hydrothermal method for visible-light photocatalysis, *J. Sci. Adv. Mater. Devices*, **2021**, *6(4)*, 516–527.

[9] T. L. Thi Le *et al.*. Designing S-scheme of TiO_2@g-C_3N_4/graphene heterojunction with enhanced photocatalytic activity under visible light: Experiments and DFT calculations, *J. Alloys Compd.*, **2024**, *995*, p. 174716.

[10] R. K. Biroju *et al.*.Graphene-ZnO Thin-Film Heterostructure-Based Efficient UV Photosensors, *ACS Appl. Electron. Mater.*, **2025,** 7(11), 4888–4897.

[11] Le Thi Thanh Lieu, Le Thi Anh, Pham To Chi, Nguyen Van Kim, Le Truong Giang, Vo Vien. Synthesis, characterization and photocatalytic performance of titanium dioxide on graphitic carbon nitride photocatalysts synthesized by hydrothermal method, *Vietnam J. Chem.*, **2019**, *57*, 411–420.

[12] D. R. Paul, S. Gautam, P. Panchal, S. P. Nehra, P. Choudhary, and A. Sharma. ZnO-modified g-C_3N_4: A potential photocatalyst for environmental application, *ACS Omega*, **2020**, *5(8*), 3828–3838.

[13] J. Tauc, Optical properties and electronic structure of amorphous ge and Si J., *Mater. Res. Bullentin*, **1968**, *3(1)*, 37–46.

.